Implementations of User Defined Shell Elements and Material Models to LS-DYNA and Their Application

J.W. Yoon and R.E. Dick
Alcoa Technical Center
100 Technical Dr., Alcoa Center, PA 15609-0001, USA
(jeongwhan.yoon@alcoa.com, robert.dick@alcoa.com)

Abstract

Robustness, accuracy and good computational performance for large scale models are some of the salient requirements for general purpose finite element programs. A new one point quadrature shell element that meets these requirements has been previously developed in the works of Cardoso & Yoon (2005). In the theory, the finite element strain-displacement matrices are described in a convective coordinate system for the efficient implementation of a physical stabilization procedure. In order to increase the computational efficiency of the shell element, in this work the resultant-stress equations are formulated by reducing dimensionality to the shell's mid-surface. In order to improve the simulation accuracy of sheet metal forming simulation utilizing commercial software, the proposed one-point quadrature element and a typical fully integrated element have been implemented to LS-DYNA using the user element interface. In addition, a plane stress yield function (Yld2000-2d, Barlat et al. (2003)) and a new anisotropic model (Yld2004-18p, Barlat et al. (2005)) that accurately describe the anisotropic behavior of aluminum alloy sheets were also implemented to LS-DYNA user material option (UMAT). Several examples including sheet forming are presented to demonstrate the element's robustness and efficiency and to verify the interface.

Introduction

The development of reduced integration shell elements has been intensively investigated by many researchers. The development for general-purpose finite element program is prompted by the need for improved performance, namely: i) robustness of the element's ability to deal with volumetric locking (Belytschko and Bindeman (1991)), and shear and membrane locking (Hughes (1978, 1980)), ii) efficiency of the element in numerical computation. Among the works, Cardoso and Yoon (2005]) recently developed a warping efficient one point quadrature shell element based on physical stabilization using a convected coordinate system and a fiber coordinate system at the nodes. In the work, the fiber coordinate system at each node warps with the element. Also, the deformation tensor derived from the convective coordinate system improves the element performance for warped configurations. The element by Cardoso and Yoon et al.(2005) has been implemented in the commercial code LS-DYNA using the User Defined Element Option. The interface allows use of any user defined element rather than the element library provided within LS-DYNA. The standard elements occasionally show poor performance in some rigid-packaging applications. By using the user defined element, improved solutions can be obtained, since element performance is directly related to the solution accuracy. The performance and efficiency of the elements are demonstrated by various linear and nonlinear examples.

Many anisotropic yield functions associated with isotropic work hardening have been proposed. Recently, a plane stress yield function, which accounts for yield stress and r-value

directionalities for every 45 degrees simultaneously was proposed by Barlat et al.(2003) (called Yld2000-2d). Also, Barlat et al.(2005) suggested a new anisotropic model (call Yld2004-18p) which takes into account more than four ears. The yield function requires experimental input data every 15 degrees (if the data is available). Thus, it can capture the detailed distributions of both r-values and yield stress anisotropies. In addition, the new model has the full three-dimensional stress tensor. Therefore, it can be applied to situations involving an arbitrary number of stress components including shell and solid models. In this work, both Yld2000-2d and Yld2004-18p models were implemented to LS-DYNA UMAT. Tensile bar test and Earing prediction were presented to validate the yield functions.

Reduced Integration Shell Theory

Displacement field

There are, in essence, four important coordinate systems for the shell element: i) Global coordinate system defined by the (x, y, z) coordinates; ii) Convective coordinate system defined at the center of the element; iii) Local coordinate system at the center of the element, with the base vectors $\hat{x}$, $\hat{y}$ and $\hat{z}$; iv) Local nodal coordinate system at each node, defined by the base vectors $\mathbf{V}_{1i}$, $\mathbf{V}_{2i}$ and $\mathbf{V}_{3i}$. A local nodal coordinate system is utilized to consider the element warping. The current position vector $\mathbf{r}$ of a generic point of the shell is defined by:

$$\mathbf{r} = \sum_{i=1}^{4} \frac{1}{4}(1+\xi_i\xi+\eta_i\eta+h_i\xi\eta)\left[\bar{\mathbf{r}}_i + \frac{\zeta}{2}a_i\mathbf{V}_{3i}\right], \tag{1}$$

where $\bar{\mathbf{r}}_i = \mathbf{r}_i(\xi,\eta,\zeta=0)$, $\mathbf{V}_{3i}$ is the unit fiber vector emanating from the mid-surface, a_i is the shell thickness at the nodes, ξ_i, η_i are defined as:

$$\boldsymbol{\xi} = \{-1 \quad 1 \quad 1 \quad -1\}^T ; \boldsymbol{\eta} = \{-1 \quad -1 \quad 1 \quad 1\}^T \tag{2}$$

and $h_i = \xi_i\eta_i$. The displacement $\mathbf{u}$ of a generic point is defined to be the difference between its current position, $\mathbf{r}$ and the reference position, $\mathbf{r}_n$

$$\mathbf{u} = N_i(\xi,\eta)\left[\bar{\mathbf{u}}_i + \frac{\zeta}{2}a_i(-\mathbf{V}_{1i}\theta_{1i} - \mathbf{V}_{2i}\theta_{2i})\right]. \tag{3}$$

Each node i is represented by the following degrees of freedom: three displacements $\bar{u}_i, \bar{v}_i$ and $\bar{w}_i$ and two local rotations θ_{1i} and θ_{2i}. In this work, Belytschko and Leviathan's approach (1994) is employed by enforcing invariance for rigid body motion by $\bar{\mathbf{u}}_i^P = \mathbf{P}_i\mathbf{u}_i$.

Strain tensor

Strains can be described by the combination of the displacement and rotation terms in the convective coordinate system by

$$\Delta\boldsymbol{\varepsilon} = \{\Delta\varepsilon_{11} \quad \Delta\varepsilon_{22} \quad \Delta\varepsilon_{33} \quad 2\Delta\varepsilon_{12} \quad 2\Delta\varepsilon_{13} \quad 2\Delta\varepsilon_{23}\}^T = \mathbf{B}_i\begin{Bmatrix}\mathbf{d}_i \\ \boldsymbol{\theta}_i\end{Bmatrix}. \ (i=1\sim4) \tag{4}$$

where, $\mathbf{d}_i = \{\bar{u}_i \quad \bar{v}_i \quad \bar{w}_i\}^T$ and $\boldsymbol{\theta}_i = \{\theta_{1i} \quad \theta_{2i}\}^T$. A co-rotational coordinate system is defined at the center of each element. To obtain the strain tensor at the co-rotational coordinate system, a

second order transformation is used to transform the strains based on the convective coordinate to the local co-rotational coordinate system:

$$\hat{\mathbf{B}}_i = \Im \mathbf{B}_i \,, \tag{5}$$

where $\Im$ is a 5×6 transformation matrix. Therefore, the constant and linear parts of the strain tensor in the co-rotational coordinate system can be obtained by utilizing Eq. (5):

$$\Delta\hat{\boldsymbol{\varepsilon}}^0 = \hat{\mathbf{B}}_{1i}^0 \begin{Bmatrix} \mathbf{d}_i \\ \boldsymbol{\theta}_i \end{Bmatrix} + \zeta \hat{\mathbf{B}}_{2i}^0 \boldsymbol{\theta}_i \tag{6}$$

$$\Delta\hat{\boldsymbol{\varepsilon}}^H = \left(\xi\hat{\mathbf{B}}_{1i}^H + \eta\hat{\mathbf{B}}_{2i}^H + \xi\eta\hat{\mathbf{B}}_{5i}^H\right)\begin{Bmatrix} \mathbf{d}_i \\ \boldsymbol{\theta}_i \end{Bmatrix} + \left(\xi\zeta\hat{\mathbf{B}}_{3i}^H + \eta\zeta\hat{\mathbf{B}}_{4i}^H\right)\boldsymbol{\theta}_i \tag{7}$$

Details of Eqs. (6) and (7) are shown in the work of Cardoso and Yoon (2005).

Resultant form

In order to obtain the continuum based resultant form equations, the shell kinematics can be described as:

$$\mathbf{u}(\xi,\eta,\tilde{z}) = \bar{\mathbf{u}}(\xi,\eta) + \frac{a}{2}\zeta\breve{\mathbf{u}}(\xi,\eta) \;\; ; \;\; \tilde{z} = \frac{a}{2}\zeta \,. \tag{8}$$

The displacement field is composed of a reference-surface $\bar{\mathbf{u}}(\xi,\eta)$ contribution and a linear dependent part along the thickness $\breve{\mathbf{u}}(\xi,\eta)$. In order to obtain the resultant-stress shell equations, the finite element equations are formulated with respect to the shell's mid-surface. For this purpose, the strain-displacement matrix for the constant field is organized as follows

$$\left(\tilde{\mathbf{B}}_i^0\right)_{11\times6} = \begin{bmatrix} \left(\tilde{\mathbf{B}}_{1i}^0\right)_{5\times6} \\ (\mathbf{0})_{5\times3} \quad \left(\tilde{\mathbf{B}}_{2i}^0\right)_{5\times3} \\ \tilde{\mathbf{B}}_{di}\,|_{1\times6} \end{bmatrix}. \tag{9}$$

For the construction of $\left(\tilde{\mathbf{B}}_{1i}^0\right)_{5\times6}$ and $\left(\tilde{\mathbf{B}}_{2i}^0\right)_{5\times3}$, a rigid body projection was applied to the strain-displacement matrices. The strain-displacement matrices for the linear terms of the resultant strains are organized in the same way:

$$\left(\tilde{\mathbf{B}}_i^H\right)_{8\times6} = \begin{bmatrix} \left(\xi\tilde{\mathbf{B}}_{1i}^H + \eta\tilde{\mathbf{B}}_{2i}^H + \xi\eta\tilde{\mathbf{B}}_{5i}^H\right)_{5\times6} \\ (\mathbf{0})_{3\times3} \quad \left(\xi\tilde{\mathbf{B}}_{3i}^H + \eta\tilde{\mathbf{B}}_{4i}^H\right)_{3\times3} \end{bmatrix} \tag{10}$$

Stiffness matrix

The stiffness matrix for the present one point quadrature shell element is a sum of the constant contribution $\mathbf{K}_{ij}^0$ and the hourglass term $\mathbf{K}_{ij}^H$. These contributions are integrated in different ways

inside the element domain. For the constant term $\mathbf{K}_{ij}^{0}$, the element stiffness matrix is obtained from the following equation:

$$\mathbf{K}_{ij}^{0} = \left(\tilde{\mathbf{B}}_{i}^{0}\right)^{T} \hat{\mathbf{D}} \left(\tilde{\mathbf{B}}_{j}^{0}\right) A \tag{11}$$

where A denotes the area of the element and is given by $A = 4\det(\mathbf{J}_0)$. The constitutive stress-strain matrix $\hat{\mathbf{D}}$ is in the resultant form after integrating through the thickness direction as follows:

$$\hat{\mathbf{D}} = \begin{bmatrix} \int_{\tilde{z}} \hat{\mathbf{C}}^{p} d\tilde{z} & \mathbf{0} & \int_{\tilde{z}} \tilde{z}\, \hat{\mathbf{C}}^{p} d\tilde{z} & \mathbf{0} & 0 \\ \mathbf{0} & \int_{\tilde{z}} \hat{\mathbf{C}}^{s} d\tilde{z} & \mathbf{0} & \mathbf{0} & 0 \\ \int_{\tilde{z}} \tilde{z}\, \hat{\mathbf{C}}^{p} d\tilde{z} & \mathbf{0} & \int_{\tilde{z}} \tilde{z}^{2}\, \hat{\mathbf{C}}^{p} d\tilde{z} & \mathbf{0} & 0 \\ \mathbf{0} & \mathbf{0} & \mathbf{0} & \mathbf{0} & 0 \\ 0 & 0 & 0 & 0 & \hat{C}^{d} \end{bmatrix}, \tag{12}$$

with $\hat{\mathrm{C}}^{d} = \delta \int_{\tilde{z}} \frac{1}{2} (\hat{\mathrm{C}}^{s}(1,1) + \hat{\mathrm{C}}^{s}(2,2)) \mathrm{d}\tilde{z}$ (δ is small value). In Eq. (12), $\hat{\mathbf{C}}^{p}$ (3x3) and $\hat{\mathbf{C}}^{s}$ (2x2) are the consistent tangent moduli of each material law which correspond to the membrane and shear terms. The Hourglass component of the stiffness matrix $\mathbf{K}_{ij}^{H}$ can be integrated analytically or numerically in the resultant mid-surface. In both cases, the stiffness matrix is obtained from the following integral:

$$\mathbf{K}_{ij}^{H} = \int_{S} \left(\tilde{\mathbf{B}}_{i}^{H}\right)^{T} \hat{\mathbf{D}} \left(\tilde{\mathbf{B}}_{j}^{H}\right) dS\,, \tag{13}$$

Internal force vector

In the one point quadrature shell element, the internal force vector is the sum of the constant and linear terms $\mathbf{F}_{i}^{0}$ and $\mathbf{F}_{i}^{H}$, respectively. The constant force vector ${}^{t+\Delta t}\mathbf{F}_{i}^{0}$ at time step $t+\Delta t$ is calculated at the element center as follows:

$${}^{t+\Delta t}\mathbf{F}_{i}^{0} = \left(\tilde{\mathbf{B}}_{i}^{0}\right)^{T} \mathbf{S}^{0} A, \tag{14}$$

where $\mathbf{S}^{0}$ is the resultant stress defined below. The resultant stress vector $\mathbf{S}^{0}$ is obtained after integrating the stresses through the thickness as follows:

$$\mathbf{S}^{0} = \int_{\tilde{z}}^{t+\Delta t} \boldsymbol{\sigma}_{l}^{0} dz \tag{15}$$

For each Gauss point through the element thickness, the stresses at time step $t+\Delta t$ are updated from the stresses at time step t. The increment of the hourglass force vector is also evaluated at the mid-point configuration:

$$\Delta\mathbf{F}_{i}^{H} = \int_{S} \left({}^{t+\Delta t/2}\tilde{\mathbf{B}}_{i}^{H}\right)^{T} \Delta\mathbf{S}^{H} dS\,, \tag{16}$$

where:

$$\Delta \mathbf{S}^{H} = \int_{\tilde{z}}^{t+\Delta t} \Delta \boldsymbol{\sigma}_l^H \, dz \,. \tag{17}$$

and:

$$\left\{\Delta \boldsymbol{\sigma}^H\right\} = \hat{\mathbf{D}} \begin{bmatrix} \left(\xi \tilde{\mathbf{B}}_{1i}^H + \eta \tilde{\mathbf{B}}_{2i}^H + \xi\eta \tilde{\mathbf{B}}_{5i}^H\right)_{5\times 6} \\ (\mathbf{0})_{3\times 3} \quad \left(\xi \tilde{\mathbf{B}}_{3i}^H + \eta \tilde{\mathbf{B}}_{4i}^H\right)_{3\times 3} \end{bmatrix} \left\{\overline{u}_i \quad \overline{v}_i \quad \overline{w}_i \quad \theta_{xi} \quad \theta_{yi}\, \theta_{zi}\right\}^T . \tag{18}$$

Finally, the hourglass force is updated into the configuration at $t+\Delta t$ as follows:

$${}^{t+\Delta t}\mathbf{F}_i^H = {}^{t}\mathbf{F}_i^H + \Delta \mathbf{F}_i^H \,. \tag{19}$$

Interface with LS-DYNA

The LS-DYNA interface is designed to accommodate full and reduced integration shell elements. For a fully integrated shell element, it is required to pass only the user-defined beta matrix (**B**) and Jacobian determinant ($|\mathbf{J}|$). LS-DYNA calculates the "Stiffness Matrix" and "Internal Force vector" as follows:

$$\mathbf{K} = \int_v \mathbf{B}^T \mathbf{C}\mathbf{B} dv \,,\ \mathbf{F} = \int_v \mathbf{B}^T \boldsymbol{\sigma} dv \ . \tag{20}$$

On the other hand, for a reduced integration element (hourglass element), it is required to pass $\mathbf{K}^{\mathrm{H}}$ and $\mathbf{F}^{\mathrm{H}}$ in addition to the beta matrix ($\mathbf{B}^{\mathrm{o}}$) and the Jacobian determinant ($|\mathbf{J}^{\mathrm{o}}|$) for the constant part. LS-DYNA constructs the following stiffness and internal force vectors:

$$\mathbf{K} = \int_v \mathbf{B}^{\mathrm{o}\,T} \mathbf{C}\mathbf{B}^{\mathrm{o}} dv + \mathbf{K}^{\mathrm{H}} ,\ \mathbf{F} = \int_v \mathbf{B}^{\mathrm{o}\,T} \boldsymbol{\sigma}^{o} dv + \mathbf{F}^{\mathrm{H}} \,. \tag{21}$$

The "***SECTION_SHELL**" card is required to be added in the input file as following (LS-DYNA User's Manual (2006), to be appear).

Constitutive Modeling

For cubic metals, there are typically enough potentially activate slip systems to accommodate any shape change. Compressive and tensile yield strengths are virtually identical and yielding is not influenced by the hydrostatic pressure. The yield surface of such materials is usually represented adequately by an even function of the principal values S_k of the stress deviator **s** suggested by Hosford (1972), i.e.,

$$\phi = |S_1 - S_2|^a + |S_2 - S_3|^a + |S_3 - S_1|^a = 2\bar{\sigma}^a \,. \tag{22}$$

The exponent a is connected to the crystal structure of the material, i.e., 6 for BCC and 8 for FCC.

Extensions of Eq. (22) based to the case of planar anisotropy are briefly summarized for a plane-stress and a general stress state. The formulation is based on two linear transformations of the stress deviator. The two linear transformations can be expressed as

$$\begin{aligned}\tilde{\mathbf{s}}' &= \mathbf{C}'\mathbf{s} = \mathbf{C}'\mathbf{T}\boldsymbol{\sigma} = \mathbf{L}'\boldsymbol{\sigma} \\ \tilde{\mathbf{s}}'' &= \mathbf{C}''\mathbf{s} = \mathbf{C}''\mathbf{T}\boldsymbol{\sigma} = \mathbf{L}''\boldsymbol{\sigma}\end{aligned} \tag{23}$$

where $\mathbf{T}$ is a matrix that transforms the Cauchy stress tensor $\boldsymbol{\sigma}$ to its deviator $\mathbf{s}$. $\tilde{\mathbf{s}}'$ and $\tilde{\mathbf{s}}''$ are the linearly transformed stress deviators and $\mathbf{C}'$ and $\mathbf{C}''$ (or $\mathbf{L}'$ and $\mathbf{L}''$) are the matrices containing the anisotropy coefficients.

For plane stress, these two linear transformations reduce to

$$\begin{bmatrix}\tilde{s}'_{xx}\\ \tilde{s}'_{yy}\\ \tilde{s}'_{xy}\end{bmatrix} = \begin{bmatrix}\alpha_1 & 0 & 0\\ 0 & \alpha_2 & 0\\ 0 & 0 & \alpha_7\end{bmatrix}\begin{bmatrix}s_{xx}\\ s_{yy}\\ s_{xy}\end{bmatrix}, \quad \begin{bmatrix}\tilde{s}''_{xx}\\ \tilde{s}''_{yy}\\ \tilde{s}''_{xy}\end{bmatrix} = \frac{1}{3}\begin{bmatrix}4\alpha_5-\alpha_3 & 2\alpha_6-2\alpha_4 & 0\\ 2\alpha_3-2\alpha_5 & 4\alpha_4-\alpha_6 & 0\\ 0 & 0 & 3\alpha_8\end{bmatrix}\begin{bmatrix}s_{xx}\\ s_{yy}\\ s_{xy}\end{bmatrix}. \tag{24}$$

Let $\tilde{S}'_i$ and $\tilde{S}''_j$ denote the principal values of the tensors $\tilde{\mathbf{s}}'$ and $\tilde{\mathbf{s}}''$ defined above. The plane stress anisotropic yield function Yld2000-2d is defined as

$$\phi = \left|\tilde{S}'_1 - \tilde{S}'_2\right|^a + \left|2\tilde{S}''_2 + \tilde{S}''_1\right|^a + \left|2\tilde{S}''_1 + \tilde{S}''_2\right|^a = 2\bar{\sigma}^a . \tag{25}$$

Note that this formulation is isotropic and reduces to Eq. (22) if $\mathbf{C}'$ and $\mathbf{C}''$ are both equal to the identity matrix. More details regarding Yld2000-2d can be obtained in Barlat et al. (2003).

For a full stress state, the linear transformations can be expressed in the most general form with the following matrices

$$\mathbf{C}' = \begin{bmatrix}0 & -c'_{12} & -c'_{13} & 0 & 0 & 0\\ -c'_{21} & 0 & -c'_{23} & 0 & 0 & 0\\ -c'_{31} & -c'_{32} & 0 & 0 & 0 & 0\\ 0 & 0 & 0 & c'_{44} & 0 & 0\\ 0 & 0 & 0 & 0 & c'_{55} & 0\\ 0 & 0 & 0 & 0 & 0 & c'_{66}\end{bmatrix}, \mathbf{C}'' = \begin{bmatrix}0 & -c''_{12} & -c''_{13} & 0 & 0 & 0\\ -c''_{21} & 0 & -c''_{23} & 0 & 0 & 0\\ -c''_{31} & -c''_{32} & 0 & 0 & 0 & 0\\ 0 & 0 & 0 & c''_{44} & 0 & 0\\ 0 & 0 & 0 & 0 & c''_{55} & 0\\ 0 & 0 & 0 & 0 & 0 & c''_{66}\end{bmatrix}. \tag{26}$$

The anisotropic yield function Yld2004-18p is defined as

$$\begin{aligned}\phi = \phi(\tilde{\mathbf{S}}', \tilde{\mathbf{S}}'') = \phi\left(\tilde{S}'_i, \tilde{S}''_j\right) = \left|\tilde{S}'_1 - \tilde{S}''_1\right|^a + \left|\tilde{S}'_1 - \tilde{S}''_2\right|^a + \left|\tilde{S}'_1 - \tilde{S}''_3\right|^a + \\ + \left|\tilde{S}'_2 - \tilde{S}''_1\right|^a + \left|\tilde{S}'_2 - \tilde{S}''_2\right|^a + \left|\tilde{S}'_2 - \tilde{S}''_3\right|^a + \left|\tilde{S}'_3 - \tilde{S}''_1\right|^a + \left|\tilde{S}'_3 - \tilde{S}''_2\right|^a + \left|\tilde{S}'_3 - \tilde{S}''_3\right|^a = 4\bar{\sigma}^a\end{aligned} . \tag{27}$$

This formulation becomes isotropic if all the coefficients c'_{ij} and c''_{ij} reduce to one. The reader is referred to Barlat et al. (2005) for additional information about this model.

The LS-DYNA provides UMAT (**U**ser **MAT**erial) option for the integration of a user defined material model. Through UMAT, Yld2000-2d and Yld2004-18p can be integrated. The main purpose of the module is to calculate the current stress as follows:

$$\boldsymbol{\sigma}_{n+1} = \boldsymbol{\sigma}_n + \Delta\boldsymbol{\sigma} = \boldsymbol{\sigma}_n + \mathbf{C}(\Delta\boldsymbol{\varepsilon} - \Delta\boldsymbol{\varepsilon}^p) = \boldsymbol{\sigma}_n + \mathbf{C}\left(\Delta\boldsymbol{\varepsilon} - \Delta\bar{\varepsilon}^p \frac{\partial\bar{\sigma}}{\partial\boldsymbol{\sigma}}\right). \tag{28}$$

The procedure to calculate Eq. (28) is described in Yoon et al. (1999) in detail. Yield function is involved when the effective stress $\bar{\sigma}$ is calculated in Eq. (28). Both Yld2000-2d (Eq. (25)) and Yld2004-18p (Eq. (27)) were incorporated in this study.

Numerical Results

The interface verification of the proposed element and constitutive modeling was conducted by performing numerical simulations on a wide spectrum of problems which are frequently used for shell element validations. The proposed element is denoted as CYSE-R (Cardoso & Yoon Shell Element-Reduced integrated) and CYSE-F (Cardoso & Yoon Shell Element-Fully integrated). Several nonlinear examples are considered in this section.

Hemispherical shell

The example is illustrated in Fig.1 in which the radius R=10.0, the thickness a=0.04, the Young's modulus E=6.825 x10^7 and the Poisson's ratio v=0.3 were used. The following boundary conditions were assumed: the bottom circumferential edge of the hemispherical is free with opposing radial point loads, F=2.0 alternating at 90 degrees. The exact displacement solution for the loaded point is 0.0924. The problem is a valuable test for the behavior of the shell when the elements are warped. As pointed out in the work of Belytschko and Leviatan (1994), a large section of this hemispherical shell rotates almost as a rigid body in response to the alternating point loads. As a result, some elements show parasitic membrane straining when warped and therefore lock. The present element shows excellent behavior in this example demonstrating the ability to deal with rigid-body motions. Comparison including CYSE and QPH (Belytschko and Leviatan (1994)) is made in Table 1.

Table 1. Hemispherical shell (results are normalized with respect to 0.0924)

Number of Elements	QPH	BWC	FISE	CYSE-R	CYSE-F
12	0.28	0.94	0.32	0.39	0.54
48	0.86	1.00	0.92	0.91	0.96
192	0.99	1.01	0.99	0.99	0.99

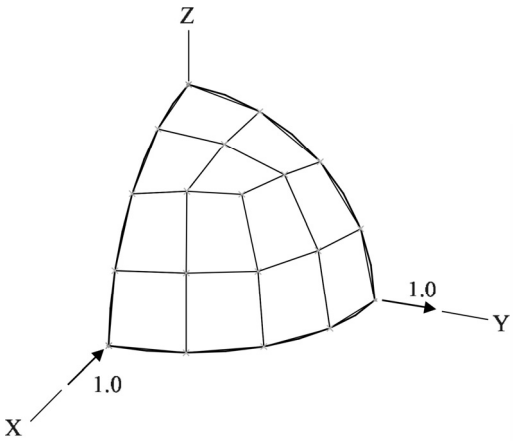

Fig.1 Hemispherical shell

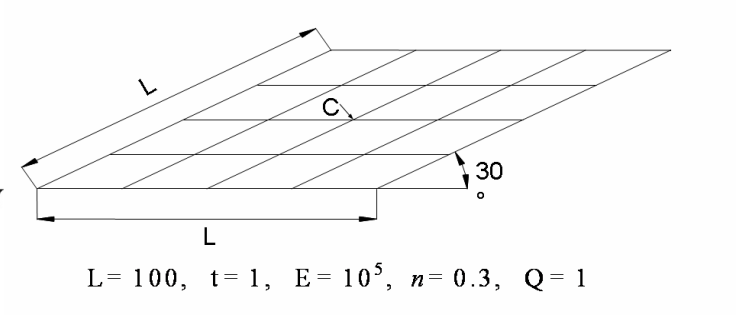

Fig.2 Schematic view for 30° skew plate

Morley's 30 skew plate

Originally proposed by Morley in 1963, this plate example is analyzed to test the sensitivity of the formulation to mesh distortions, as well as the ability to avoid any locking phenomenon. The geometry possesses a low thickness to length ratio (1/100) and the elements are uniformly distorted. The plate is simply-supported and subjected to a uniform pressure Q. The data for the problem is based on the work of Andelfinger and Ramm (1993). Fig. 2 presents the geometry of the Morley's skew plate. In this example, length L=100.0, thickness a=1.0, Young's modulus $E=10^5$, Poisson's ratio v=0.3 and the uniform pressure Q=1.0. Table 2 presents the normalized displacement at the center of the plate (C) compared with MITC4 (Dvorkin and Bathe (1984)).

Table 2. Normalized Displacement at the Center of the Plate

Elements per Side	MITC	BWC	FISE	CYSE-R	CYSE-F
4	0.88	1.16	0.95	0.97	0.88
8	0.86	1.15	0.95	0.94	0.87
16	0.94	1.13	0.98	0.96	0.93
32	0.98	1.12	1.00	0.99	0.99

The Kirchhoff reference solution is 4.455. The present formulation leads to excellent results. Mesh convergence to the reference solution is achieved for 32 elements per side as shown in Table 4.

Torsion of a flat plate strip

The purpose of this example is to demonstrate the performance of the element in warping and rotation and, at the same time, to illustrate its robustness. A torsional moment is applied to the end of the initially flat plate strip, leading to a relative torsional rotation of 180°. It was reported that reduced integrated elements with artificial hourglass control (for example, LS-DYNA Element Library of 2 and 10, ABAQUS S4R) exhibit hourglass behaviors, while typical fully integrated elements have difficulty in rotating the full 180 degrees (for example, LS-DYNA Element Library of 16, MARC Element Library of 75). The input data are, for the material

properties, $E = 12\times10^6$ and $\nu = 0.3$, and for the geometry, the length $L = 1.0$, the width $W = 0.25$ and the thickness $a = 0.1$. The initial and deformed mesh configurations are shown in Fig.3. It can be seen that the present element performs well with excellent warping behavior.

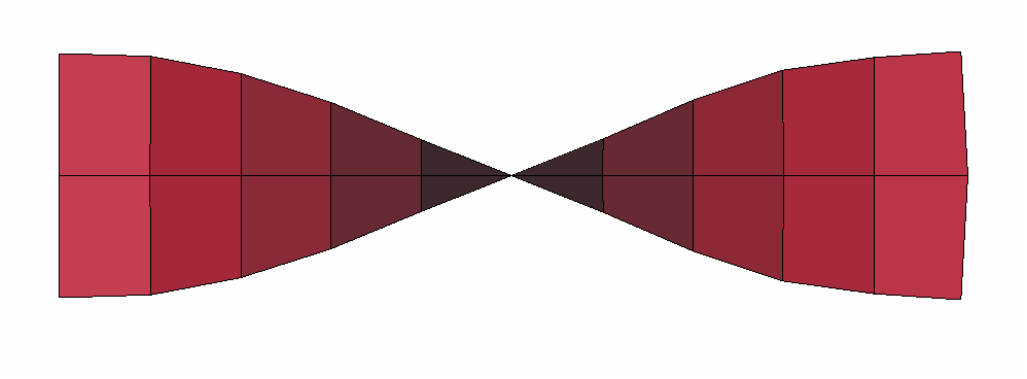

Fig.3 Torsion of a plate

Uniaxial tensile specimen

The geometry of the plane stress tensile bar is shown in Fig.4(a). The tensile bar has a thickness of 0.0100 inch and a cross-sectional area of 0.005 in^2. The material is an anisotropic material with isotropic hardening based on Yld2000-2d (Barlat et al. (2003)) using LS-DYNA UMAT. Young's modulus is 10 million psi and Poisson's ratio is 0.33. The Voce coefficients are *A*=49136, B=13106, and *C=35.56*. Displacement boundary conditions at the end of the bar are imposed using a rigid body. A total displacement of 0.15 inches is achieved in 200 equal size increments. The deformed shape and effective plastic strain contours after the onset of necking are shown in Fig.4(b). The predicted r-values at 90 degrees to the rolling direction are provided in Table 3. The theoretical r-value is 1.62.

Table 3. r-value for Uniaxial Tensile Specimen

	BWC	FISE	CYSE-R	CYSE-F
r-value	1.622	1.618	1.624	1.619

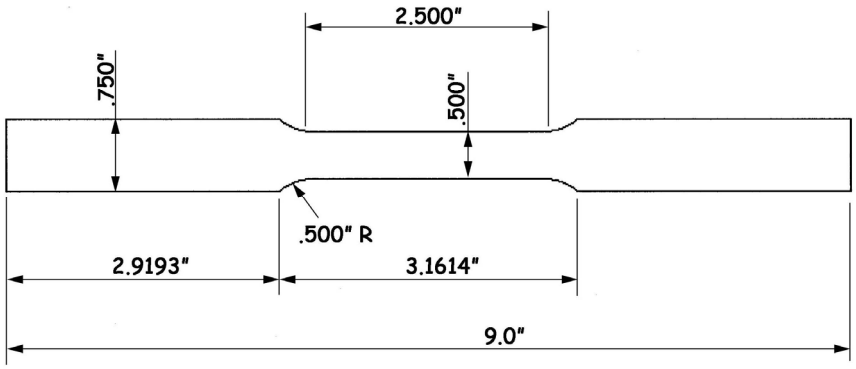

(a)

(b)

Fig.4Geometry of uniaxial tensile specimen (b) Effective plastic strain contours of uniaxial tensile specimen at onset of necking.

Mini-die earing simulation

The cup drawing test simulation with a circular punch and blank is one of most popular tests to verify the planar anisotropic behavior through the prediction of the earing profile. In the cylindrical cup-drawing test, the material undergoes compressive deformation in the flange area due to the circumferential contraction. Some stretching occurs in the radial direction of a cup. This test was simulated for an imaginary alloy sheet (called FM8) based on the proposed shell element and Yld2004 from Barlat et al. (2005) using LS-DYNA UMAT interface. Assuming isotropic hardening, the yield function coefficients are kept constant during the simulation. The mini-die geometry for the analysis is as follows:

Punch diameter:	D_p = 35.560 mm (1.4 inch)
Punch profile radius:	r_p = 2.286 (0.09 inch)
Die opening diameter:	D_d = 36.576 mm (1.44 inch)
Die profile radius:	r_d = 2.286 mm (0.09 inch)
Blank radius:	D_b = 59.385 mm (2.338 inch)

For the FM8 material, the r-value distribution is assumed to have double curvature to understand its effect on the earing profile. Figure 5(a) shows the normalized yield stress and r-value anisotropies, predicted from Yld2004. In the work of Yoon et al. (2006), it is proven that the earing profile is a mirror image of the r-value profile with respect to 90 degrees. Considering the r-value plot in Fig.6(a), eight ears are anticipated for the FM8 material. Fig.5(b) shows the deformed shape right before the sheet leaves die. It is shown that eight ears are well predicted with the present shell element. The earing profile is plotted in Fig.5(c).

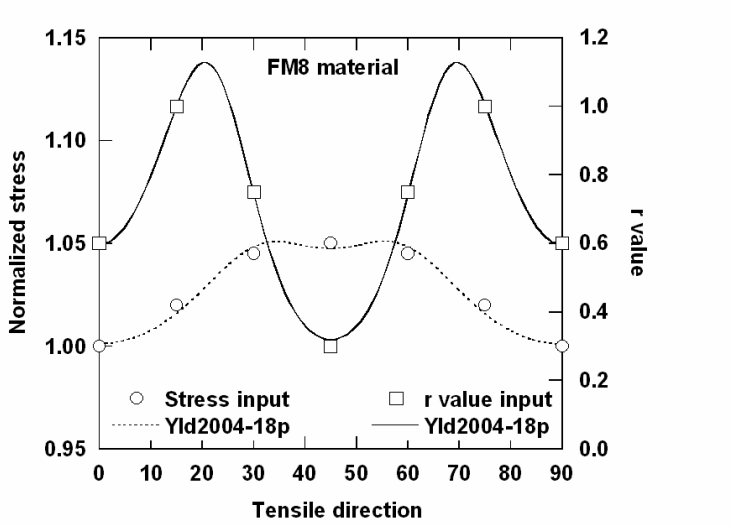

(a)

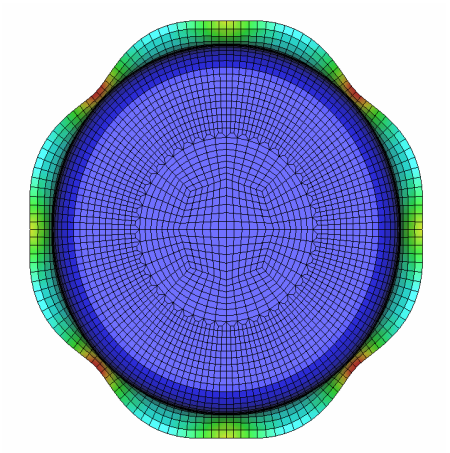

(b)

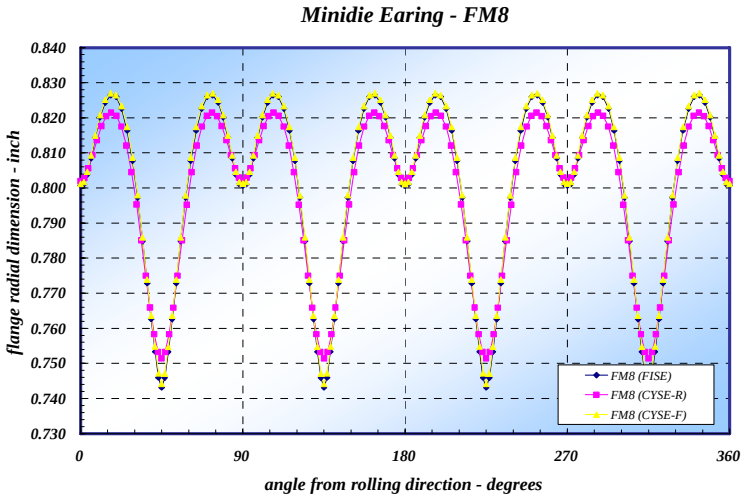

(c)

Fig.5 (a) Yield stress and r-value plot for FM8 material (b) Thickness strain contour (c) Earing profile

Summary

A one point quadrature shell element utilizing physical stabilization based on a convective coordinate system has been implemented in LS-DYNA using the User Element interface for general purpose nonlinear applications. The implemented resultant shell is computationally efficient compared to the volumetric form. The element based fiber vector is proven to be efficient and robust for severe warping. Several examples demonstrate the accuracy and robustness of the proposed element. An accurate finite element simulation can be achieved by using the proposed element. Also, Yld2000-2d and Yld2004-18p were successfully implemented into the LS-DYNA UMAT subroutine. The anisotropic properties were best captured by Yld2004-18p. The Yld2004-18p is capable of predicting more than four ears.

Acknowledgement

The authors are thankful for Drs. John Hallquist (LSTC) and Thomas Borrvall (Engineering Research AB) for the strong collaboration work to implement the user-defined shell element and material to LS-DYNA. LS-DYNA, LS-OPT, and LS-PrePost are registered trademarks of Livermore Software Technology Corporation.

References

Andelfinger, U. and Ramm, E., EAS-elements for two dimensional, three-dimensional plate and shell structures and their equivalence to HR-elements, *IJNME*, **36**, 1131 (1993).

Barlat, F., Aretz, H., Yoon, J.W., Karabin, M.E., Brem, J.C. and Dick, R.E., Linear transformation based anisotropic yield function, *Int. J. Plasticity*, **21**, 1009 (2005).

Belytschko, T and Bindeman, L.P., Assumed strain stabilization of the 4-node quadrilateral with 1-point quadrature for nonlinear problems, *Computer Methods in Applied Mechanics and Engineering*, **88**, 311 (1991).

Belytschko, T and Leviathan, I., Physical stabilization of the 4-node shell element with one point quadrature, *Computer Methods in Applied Mechanics and Engineering*, **113**, 321 (1994).

Cardoso, R.P.R., Yoon, J.W., One point quadrature shell elements for sheet metal forming analysis, *Arch. Comput. Meth. Engrg*.,12, 3-66 (2005)

Dvorkin, E.N. and Bathe, K.J., A continuum mechanics based four-node shell element for a general nonlinear analysis, *Engrg. Comput.*, **1**, 77 (1984).

Hosford, W.F., A generalized isotropic yield criterion. J. Appl. Mech. Trans. ASME, 39, 607–609 (1972).

Hughes T.J.R., Cohen M, Haroun M., Reduced selected integration techniques in finite element analysis of plates, *Nuclear Engineering and Design*, **46**, 203 (1978).

Hughes T.J.R.., Generalization of selective integration procedure to anisotropic and nonlinear media, *International Journal for Numerical Methods in Engineering*, **15**, 1413 (1980).

Yoon, J. W., Yang, D. Y. and Chung, K.. Elasto-plastic finite element method based on incremental deformation theory and continuum based shell elements for planar anisotropic sheet materials. Comput. *Methods in Appl. Mech. & Eng.*, **174**, 23-56 (1999).

Yoon, J.W., Barlat, F., Dick, R.E. and Karabin, M.E., Prediction of six or eight ears in a drawn cup based on a new anisotropic yield function, *Int. J. Plasticity*, 22, 174 (2006).